Supporting Information

Stacking Dependent Piezoelectric Response of Bilayer and Heterobilayer Group-IV Monochalcogenides under Applied External Strain

Kevin Tran [a] *and Michelle J.S. Spencer*[a] *

[a] School of Science, RMIT University, GPO Box 2476, Melbourne, Victoria 3001, Australia.

*Author to whom any correspondence should be addressed. Email: michelle.spencer@rmit.edu.au

Table S1 Lattice constants (Å) of the MX monolayers and heterobilayers.

	Lattice Constant (***a***)	Lattice Constant (***b***)
GeS	3.66	4.44
GeSe	3.94	4.39
SnS	4.02	4.44
SnSe	4.23	4.54
GeS/GeSe	3.80	4.42
GeS/SnS	3.84	4.44
GeS/SnSe	3.95	4.49
GeSe/SnS	3.98	4.14
GeSe/SnSe	4.08	4.46
SnS/SnSe	4.13	4.49

Table S2 Calculated relative energies of the MX bilayers and heterobilayers in different stacking arrangements.

	Total Energies (eV)			
	AA	AB	AC	AD
GeS/GeS	0.12	0.06	0	0.16
GeSe/GeSe	0.03	0.05	0	0.16
SnS/SnS	0.15	0.06	0	0.22
SnSe/SnSe	0.10	0.03	0	0.20
GeS/GeSe	0.09	0.05	0	0.14
GeS/SnS	0.15	0.06	0	0.19
GeS/SnSe	0.14	0.03	0	0.18
GeSe/SnS	0.13	0.04	0	0.13
GeSe/SnSe	0.08	0.03	0	0.16
SnS/SnSe	0.13	0.03	0	0.19

Table S3 Lattice mismatch of the heterobilayers

Bilayer	Lattice Mismatch (%)
GeS/SnSe	7.3
GeS/SnS	4.8
GeSe/SnSe	3.7
GeS/GeSe	3.6
SnS/SnSe	2.6
GeSe/SnS	1.0

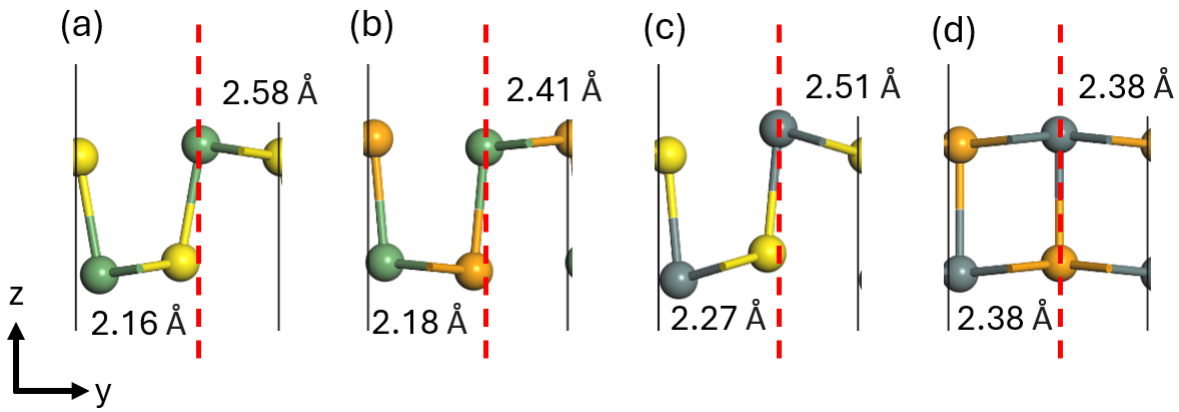

Fig. S1 Relative position of the M and X atoms along the armchair direction for monolayer (a) GeS, (b) GeSe, (c) SnS and (d) SnSe with a 6% compressive strain.

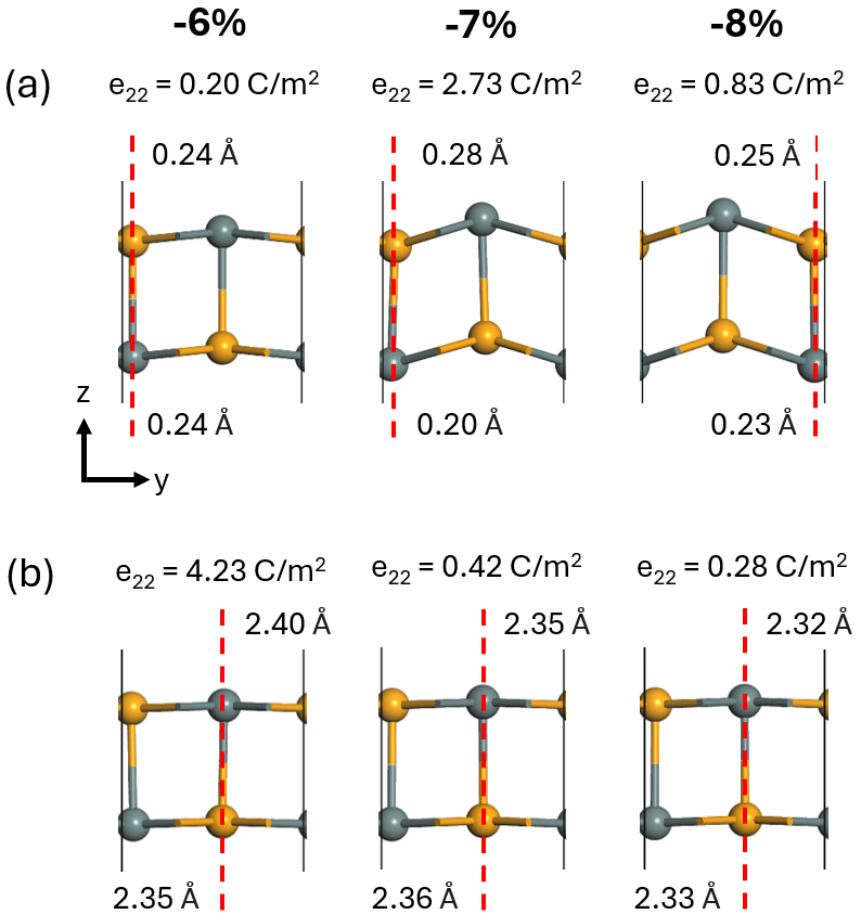

Fig. S2 Relative position of the M and X atoms along the armchair direction for monolayer SnSe upon (a) biaxial and (b) uniaxial compressive strain of -6% to -8%.

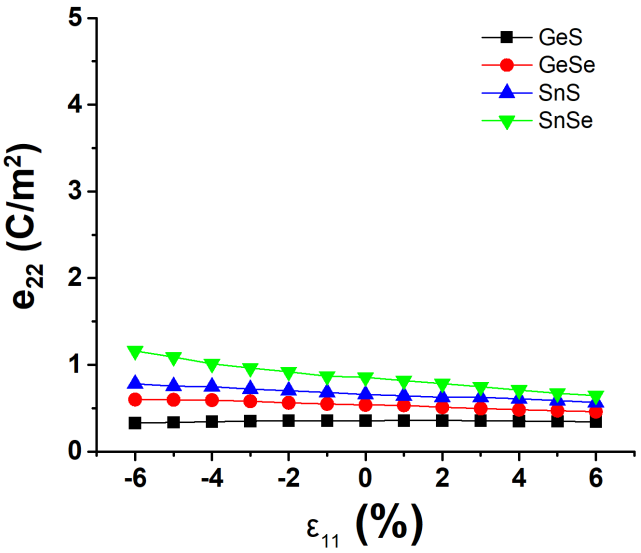

Fig. S3 Piezoelectric constant, e_{22}, of monolayer GeS, GeSe, SnS and SnSe under applied uniaxial strain along the zigzag direction.

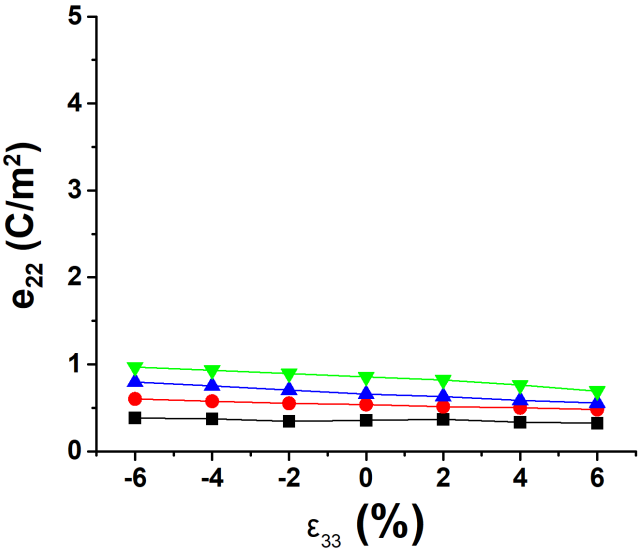

Fig. S4 Piezoelectric constant, e_{22}, of monolayer GeS, GeSe, SnS and SnSe under applied uniaxial strain along the *c*-direction.

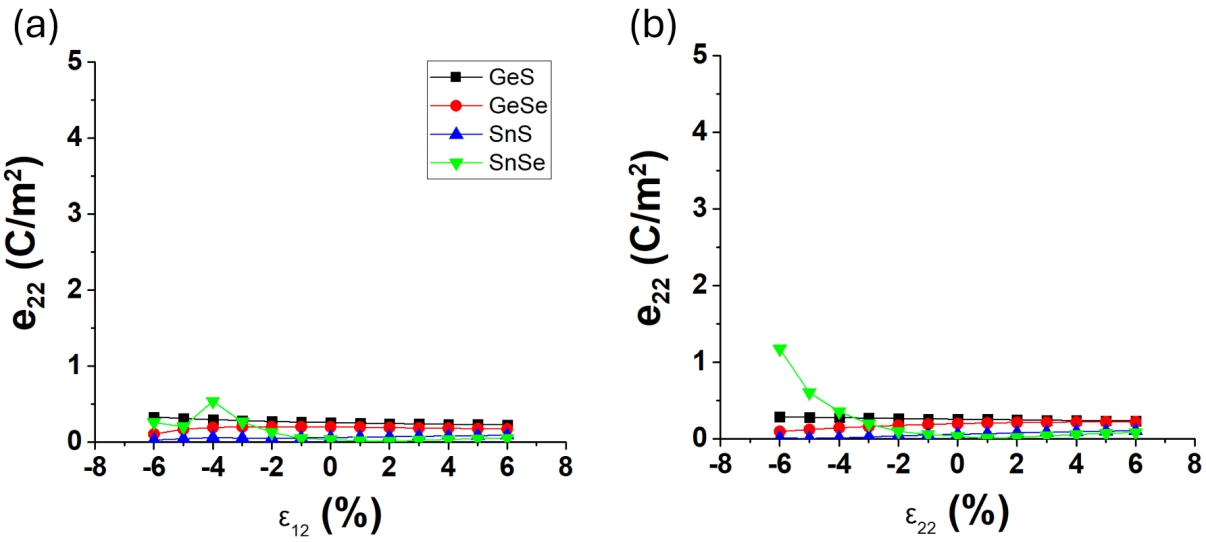

Fig. S5 Piezoelectric, e_{21}, of monolayer GeS, GeSe, SnS and SnSe under applied (a) biaxial and (b) uniaxial strain.

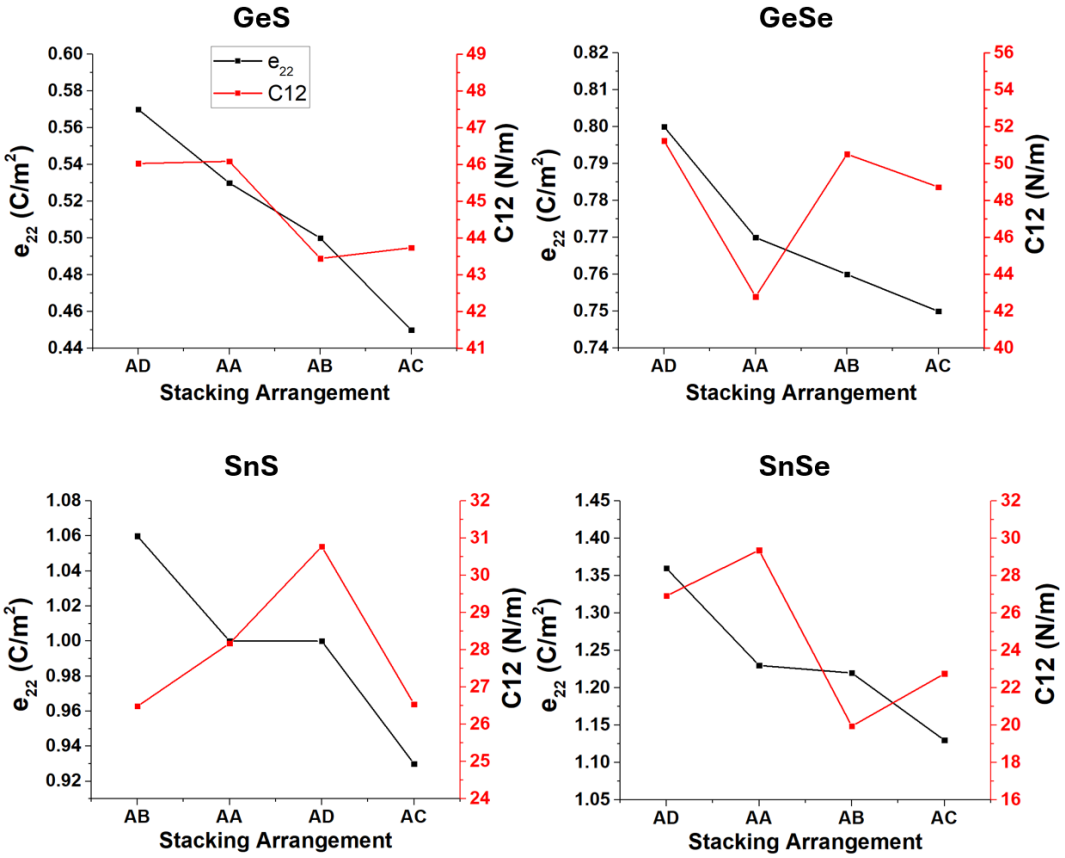

Fig. S6 Calculated e_{22} and C_{12} values of bilayer group-IV monochalcogenides in different stacking arrangements.

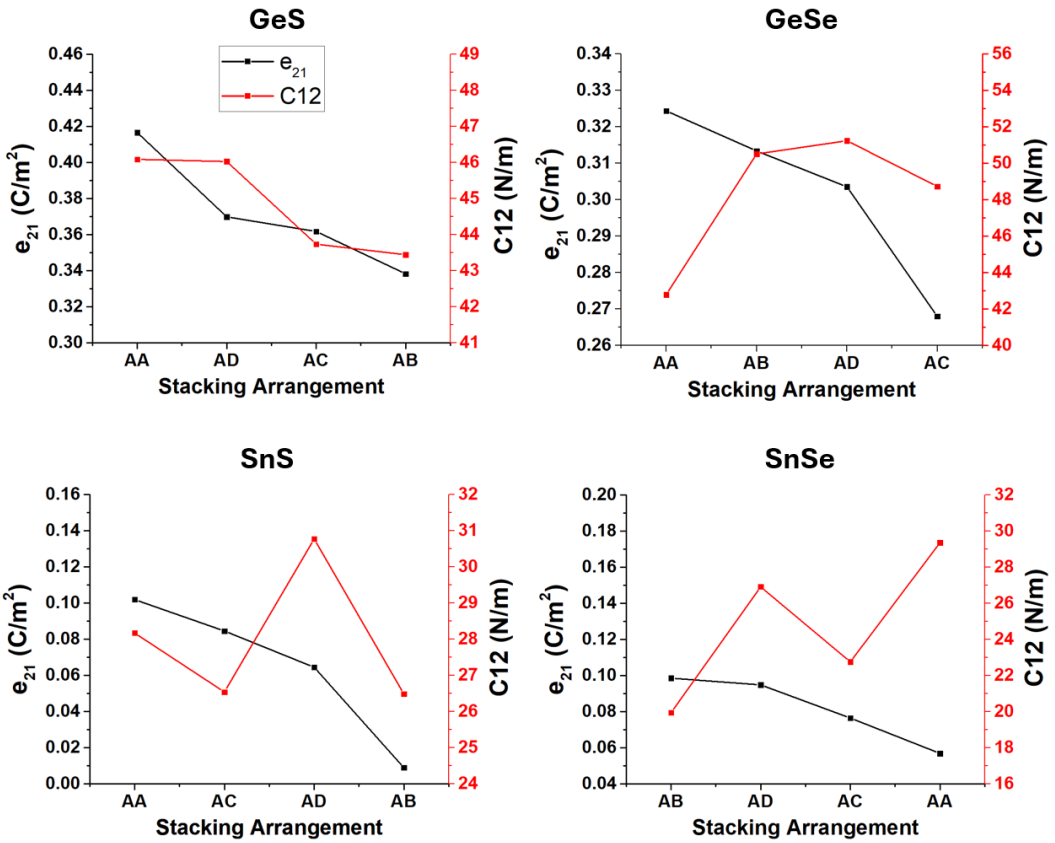

Fig. S7 Calculated e_{21} and C_{12} values of bilayer group-IV monochalcogenides in different stacking arrangements.

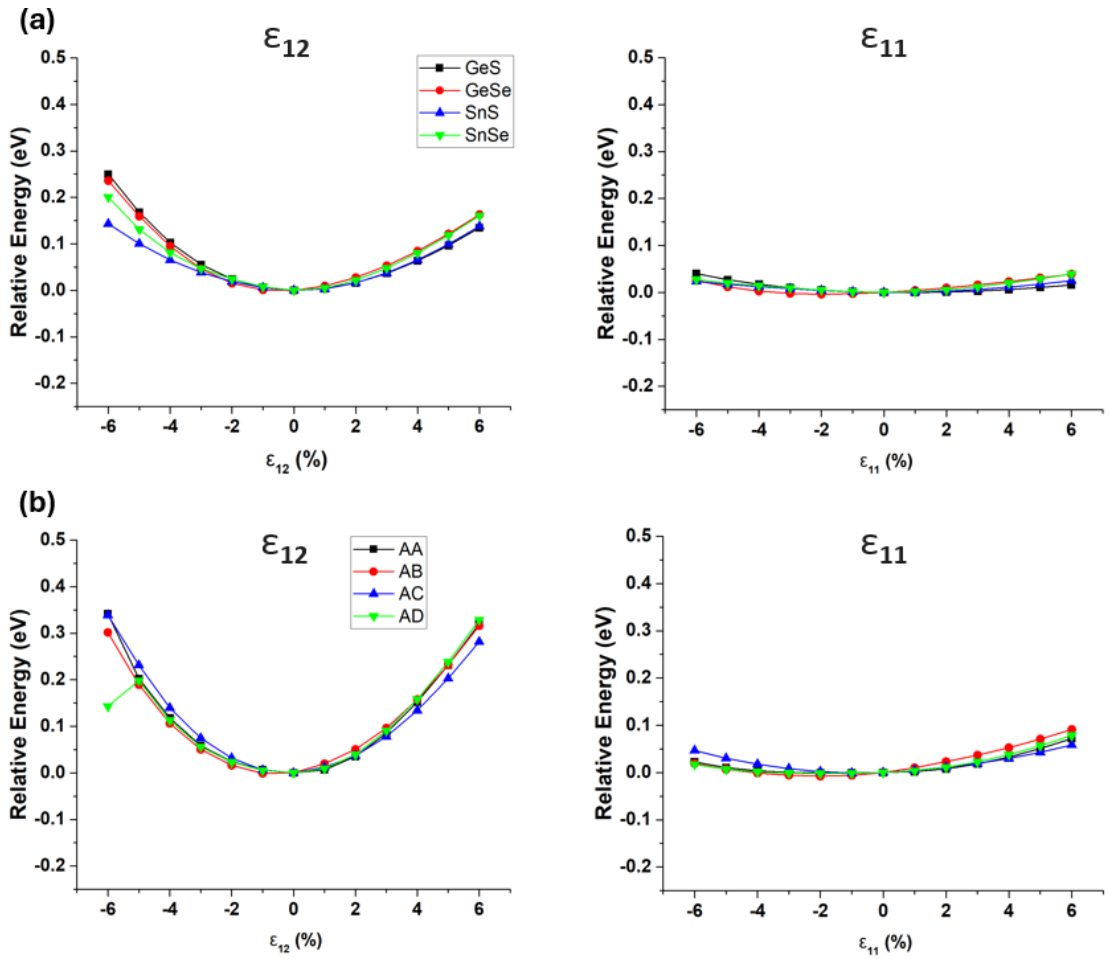

Fig S8. Relative energies of the group-IV monochalcogenide (a) monolayers and (b) bilayers under applied biaxial (ε_{12}) and uniaxial (ε_{11}) strain

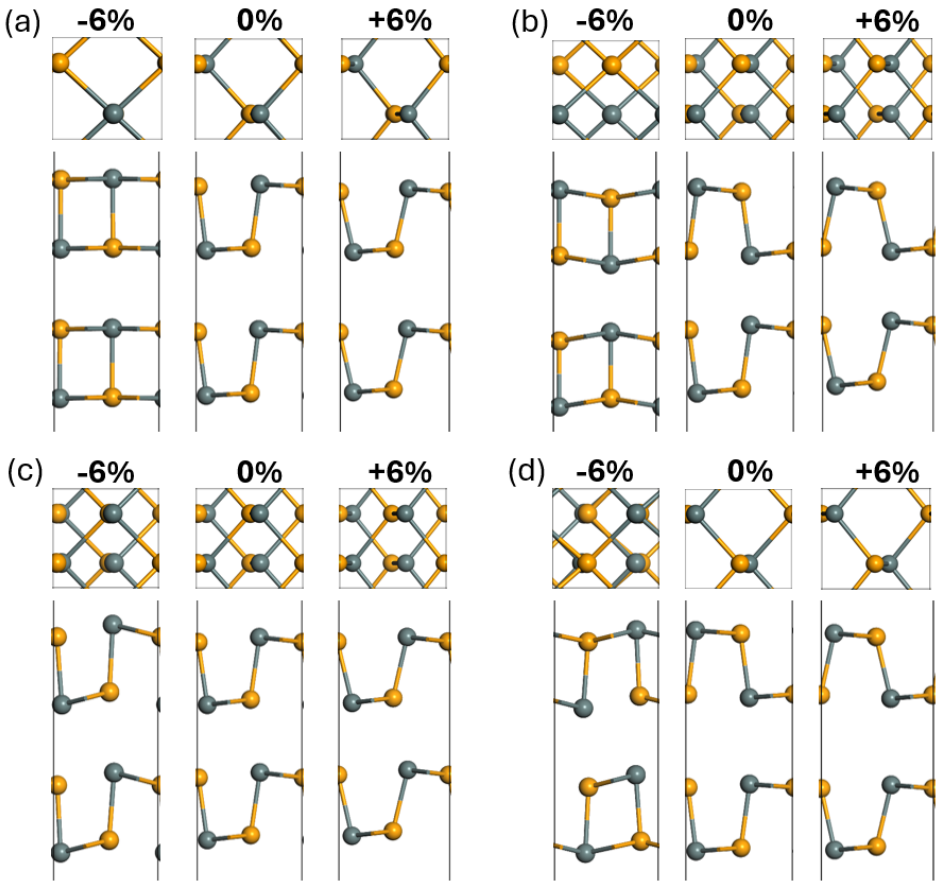

Fig. S9 Optimised structures of bilayer SnSe under applied biaxial strain in the (a) AA, (b) AB, (c) AC and (d) AD stacking arrangements. The grey and orange colours represent the Sn and Se atoms, respectively.

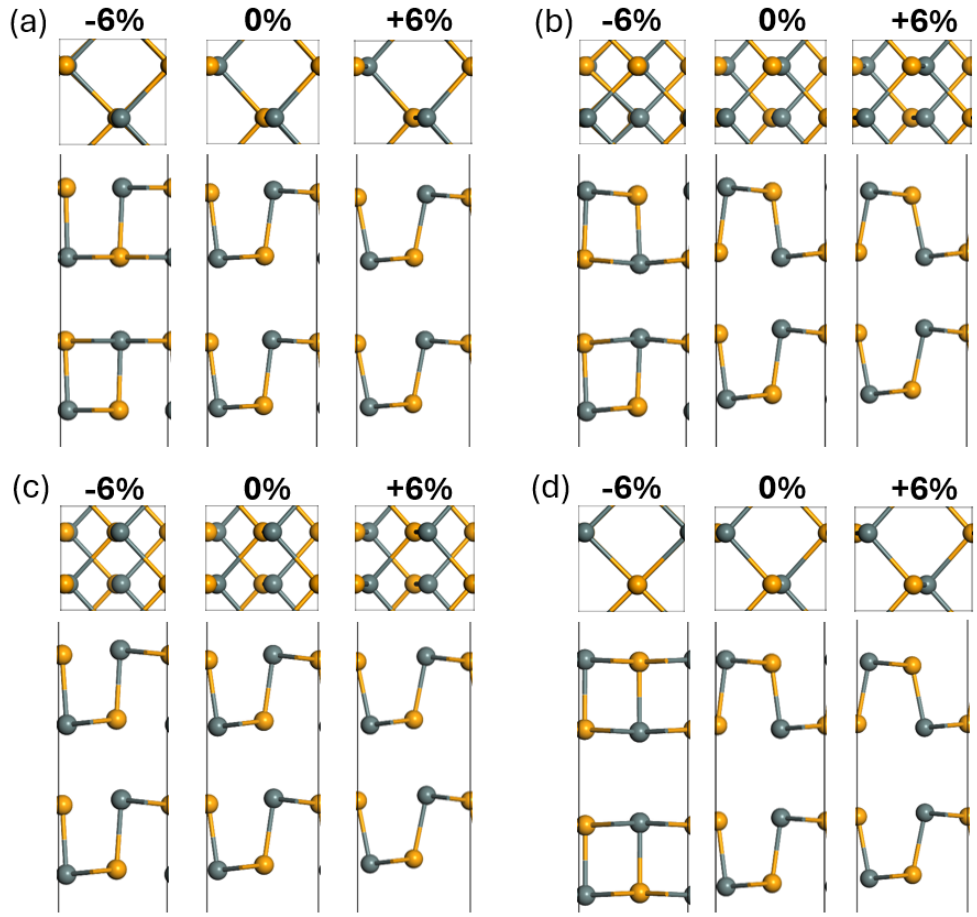

Fig. S10 Optimised structures of bilayer SnSe under applied uniaxial strain (armchair direction) in the (a) AA, (b) AB, (c) AC and (d) AD stacking arrangements.

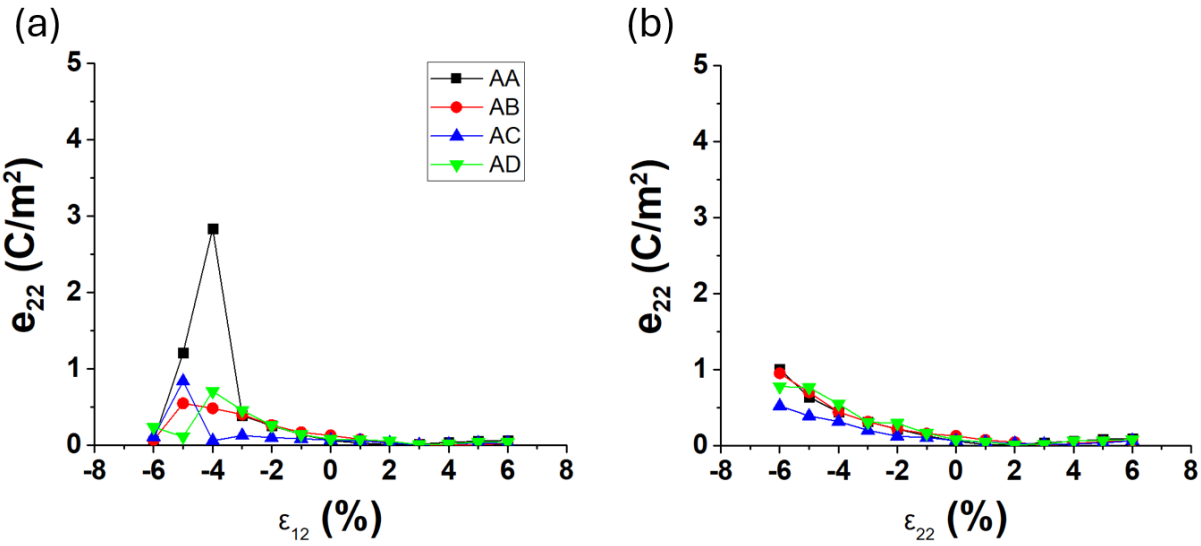

Fig. S11 Piezoelectric, e_{21}, of bilayer SnSe under applied (a) biaxial and (b) uniaxial strain.

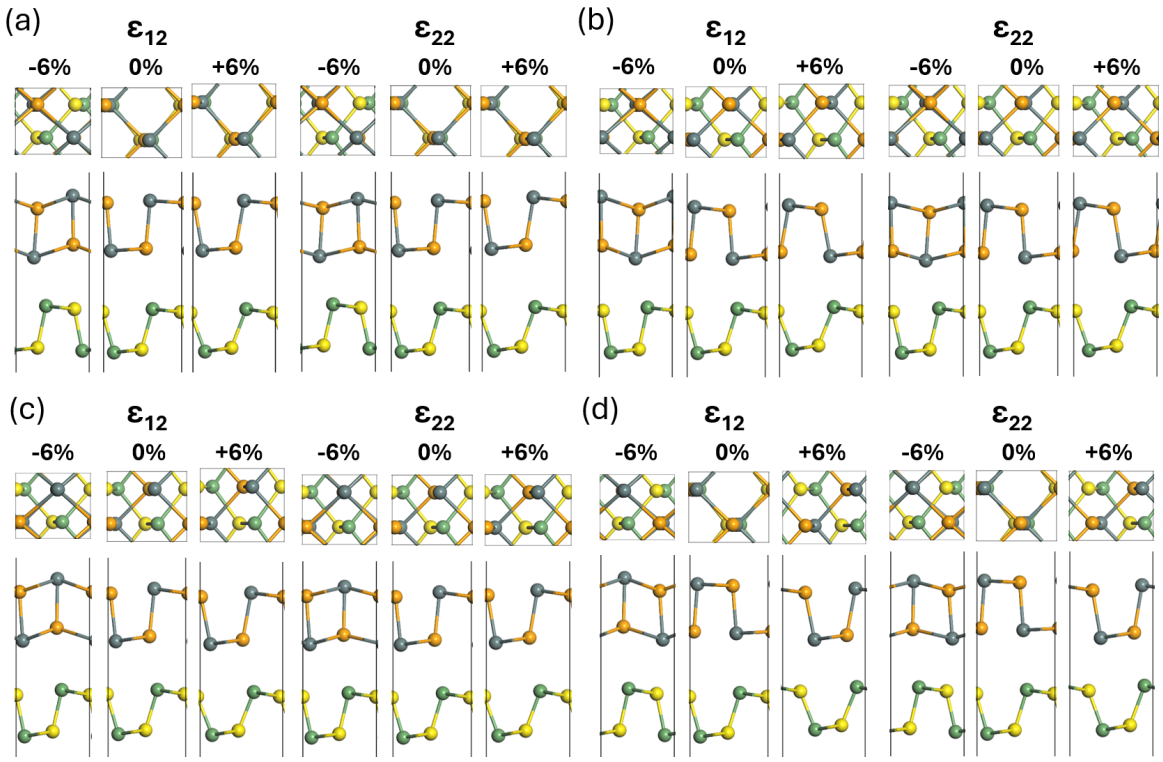

Fig. S12 Optimised structures of the GeS/SnSe heterobilayer under applied biaxial (ε_{12}) and uniaxial (ε_{22}) strain in the (a) AA, (b) AB, (c) AC and (d) AD stacking arrangements. The grey, green, orange and yellow colours represent the Sn, Ge, Se and S atoms, respectively.

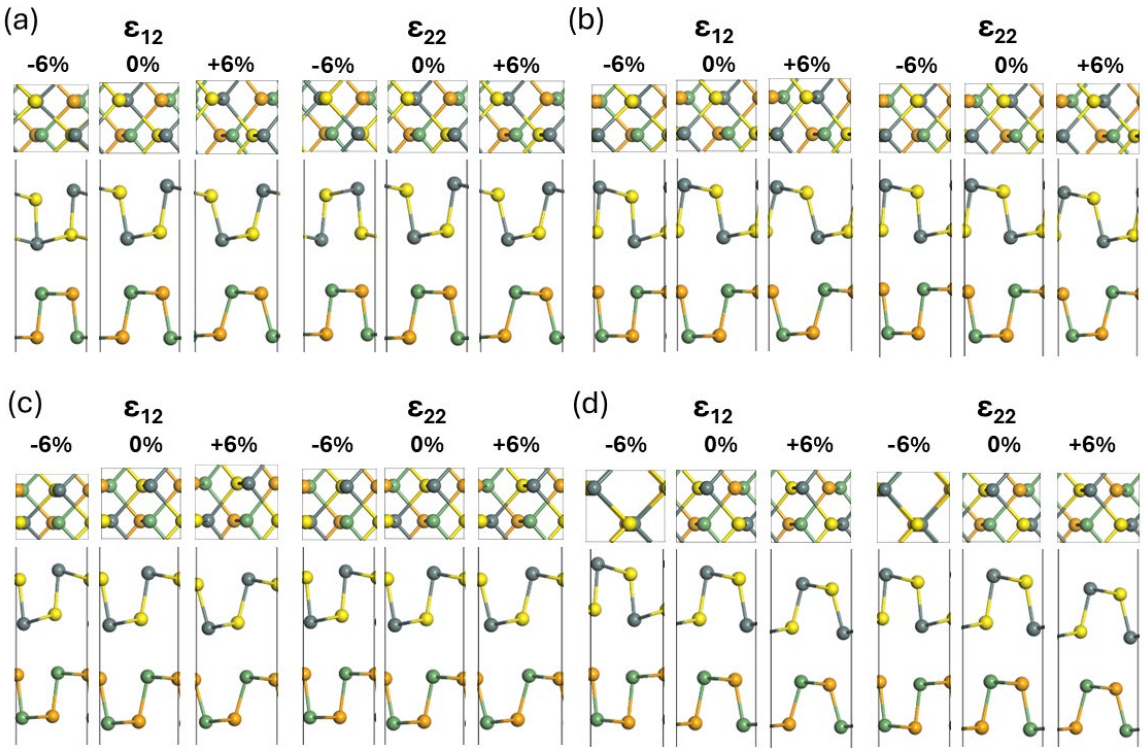

Fig. S13 Optimised structures of the GeSe/SnS heterobilayer under applied biaxial (ε_{12}) and uniaxial (ε_{22}) strain in the (a) AA, (b) AB, (c) AC and (d) AD stacking arrangements.

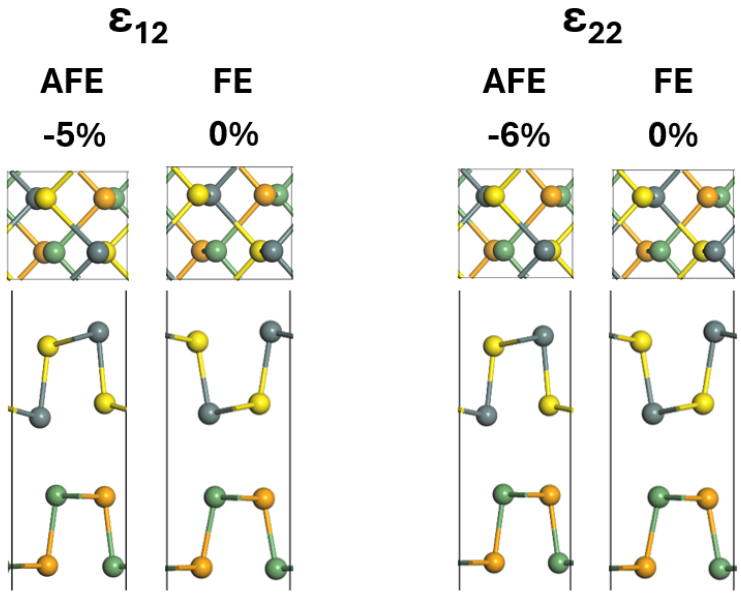

Fig. S14 FE and AFE states of the AA-stacked GeSe/SnS heterobilayer after biaxial and uniaxial compressive strain.

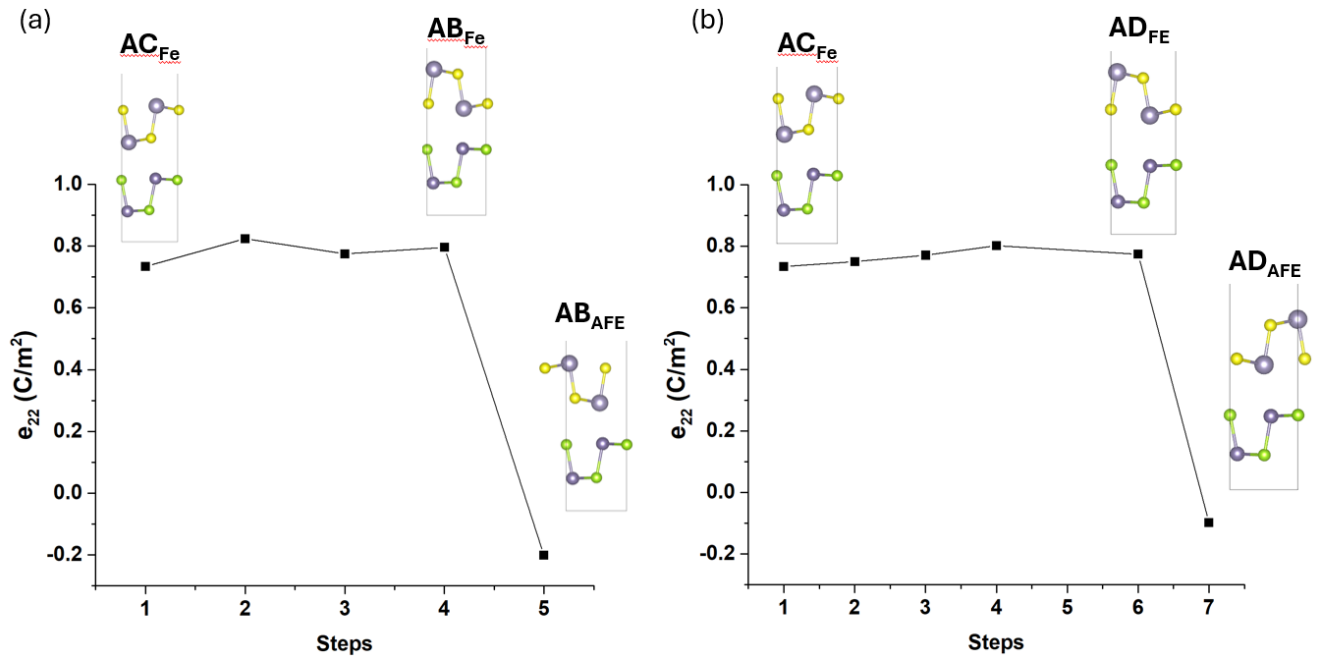

Fig. S15 Ferroelectric to antiferroelectric sliding pathway of heterobilayer GeSe/SnS from (a) $AC_{Fe} - AB_{AFE}$ to (b) $AC_{Fe} - AD_{AFE}$.

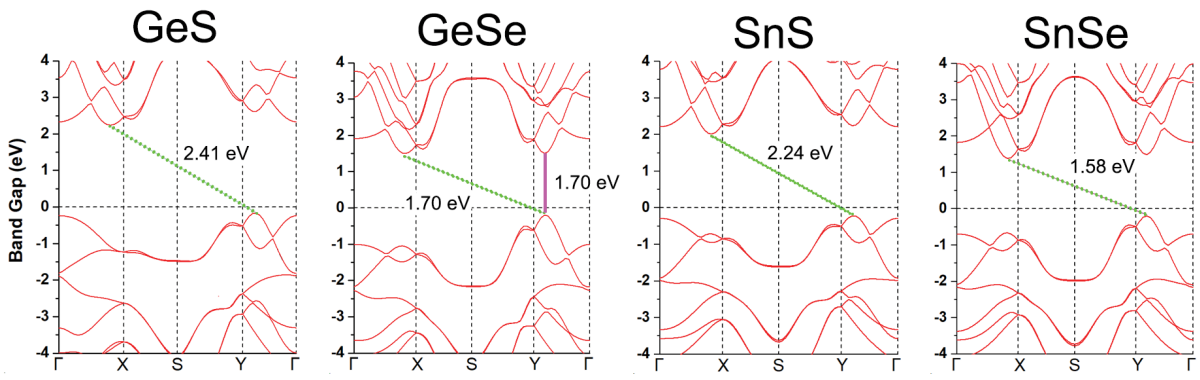

Fig. S16 Band structures of the optimised MX monolayers. The green and pink lines represent the indirect and direct band gaps, respectively.

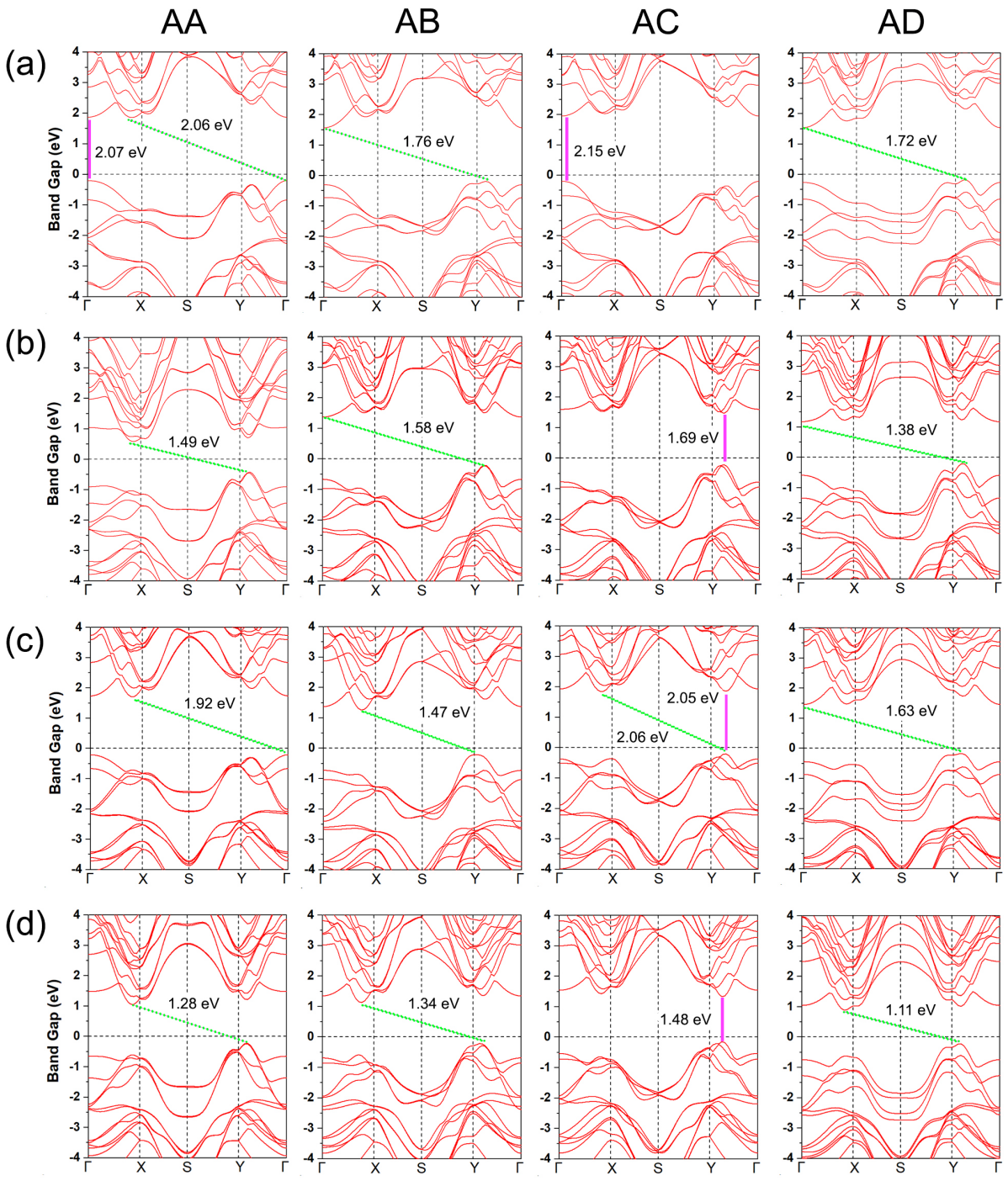

Fig. S17 Band structures of the optimised MX monolayers. The green and pink lines represent the indirect and direct band gaps, respectively.